**Supporting Information**

# A Superprotein Triangle Driven by Nickel(II) Coordination: Exploiting Non-Natural Metal Ligands in Protein Self-Assembly

Robert J. Radford, and F. Akif Tezcan
University of California, San Diego, 9500 Gilman Dr., MC 0356, La Jolla, CA 92093-0356

## Site Directed Mutagenesis and Protein Expression/Purification/Characterization

Site directed mutagenesis was performed on the pETc-b562 plasmid (denoted as wild-type)[1] using the QuikChange kit (Stratagene) and employing primers obtained from Integrated DNA Technologies. The mutant plasmids were transformed into XL-1 blue *E. coli* cells and purified using the QIAprep Spin Miniprep kit (Qiagen). Four rounds of mutagenesis were executed to obtain the final mutant W59C R62A H63A D66H K77H (hereafter referred to as MBP). Sequencing of the mutant plasmid was performed at the UCSD Moores Cancer Center.

The mutant plasmid isolated from XL-1 blue cells was transformed into BL21(DE3) *E. coli* cells along with the *ccm* heme maturation gene cassette plasmid, pEC86.[3] Cells were plated on LB agar, containing 100 μg/ml ampicillin and 34 μg/ml chloramphenicol, and grown overnight. LB medium was then inoculated from these colonies and allowed to incubate for 16 hours at 37$^{o}$ C, with rotary shaking at 250 rpm. No induction was necessary.

Mutant-expressing cells were sonicated, brought to pH 5 with the addition of HCl, and centrifuged at 16,000 g, 4$^{o}$ C, for 1 hr. The protein was then purified by ion-exchange chromatography on a CM-Sepharose matrix (Amersham Biosciences) using a NaCl gradient in sodium acetate, pH 5. After exchange into sodium phosphate, pH 8, the protein was further purified using an Uno-Q (BioRad) anion exchange column on a DuoFlow chromatography workstation (BioRad) using a NaCl gradient. Protein purity was determined by SDS-PAGE gel electrophoresis. Verification of mutations was made through MALDI mass spectrometry (mass of MBP = 12137 amu, mass of MBP-Phen1 = 12376 amu).

## Synthesis of Iodoacetamido-1,10-Phenanthroline (IA-Phen)

As a precursor, iodoacetic acid anhydride was freshly prepared by adding 2.64 g (12.8 mmol) of DCC to a stirred solution of 5.0 g (26.8 mmol) iodoacetic acid in 75 mL of ethyl acetate. Dicyclohexylurea precipitates immediately, but the mixture was allowed to stir for 2 hrs in the dark. The dicyclohexylurea was removed by filtration and the resulting solution was evaporated to dryness. 0.5 g (2.56 mmol) of 5-amino-1-10-phenanthroline (Polysciences) was dissolved in 90 mL of acetonitrile with slight heating. To this stirred solution, the iodoacetic acid anhydride dissolved in 10 mL of acetonitrile was added. The mixture was allowed to react in the dark overnight. The precipitated product was isolated by filtration and washed with cold 5% sodium bicarbonate and water and dried *in vacuo*. Both the ESI MS and NMR spectra correspond to previously reported literature values.[6] (Yield: 75%)

## Functionalization of MBP with IA-Phen and iodoacetic acid

A solution of 0.3 mM MBP in degassed 0.1 M Tris buffer (pH 7.75) was treated with a 10-fold excess of DTT. The protein was allowed to reduce for a period of 1 hr. The protein is then dialyzed against 2 L of degassed 0.1 M Tris buffer (pH 7.75) under an inert atmosphere to remove DTT. A 10-fold excess of IA-Phen or iodoacetic acid was dissolved in 2 mL of degassed DMF and added dropwise to the protein solution over the course of 1 min. The mixture was

allowed to react in the dark at 4° C overnight, after which excess free label was removed using a 10-DG gel filtration column (Biorad). The labeled protein (MBP-Phen1, Figure S1 or carboxymethyl-MBP (CM-MBP)) was dialyzed against 2 L of 0.01 M sodium phosphate (pH 8) and subsequently purified on an Uno-Q anion-exchange column using an NaCl gradient. The purity of functionalized protein was determined by MALDI mass spectrometry and SDS-PAGE electrophoresis. (Labeling yield: 60-95%)

**Equilibrium Unfolding** (Figure S2 and Table S1)

5 mL of an unfolded protein (CM-MBP or MBP-Phen1) solution containing 2 μM of protein and 1 mM of $Ni^{2+}$ or EDTA was freshly prepared in ~ 7.5 M guanidine HCl (GuHCl) in 20 mM Tris buffer (pH 7). In parallel, 3 mL of a folded protein solution containing 2 μM protein in 20 mM Tris buffer (pH 7) and 1 mM $Ni^{2+}$ or EDTA was prepared. The unfolded protein stock was titrated into the folded protein stock using an autotitrator (Microlab 500 Series), keeping the sample volume constant at 2 mL; the unfolding/folding reaction was monitored by CD spectroscopy (222 nm) on an Aviv 215 spectrometer. For every titration point, the solution was allowed to stir for 30 sec in order to reach equilibrium. This procedure was repeated for a minimum of 20 points covering a GuHCl range of 0.1-6.5 M. GuHCl concentrations were calculated using the refractive indices of the folded and unfolded protein stock solutions.[7] Unfolding data were fit using Kaleidagraph (Synergy Software) assuming a simple two-state folding/unfolding equilibrium as described by Pace (Figure S2 and Table S1).[8]

**$Ni^{2+}$ Binding Titrations** (Figure S3)

All absorption spectra were obtained on an HP 8452A spectrophotometer. MBP-Phen1 concentration was determined based on heme absorption at λ = 415 nm (ε = 0.148 $\mu M^{-1}$ $cm^{-1}$).[9] A 1 mL solution of MBP-Phen1 in 20 mM Tris buffer (pH 7) was freshly prepared from a concentrated stock using Hamilton syringes. To this solution, successive aliquots of a 500 μM $NiCl_2$ stock solution in 20 mM Tris (pH 7) were added. Binding of Ni to the Phen group was monitored by the distinct red shift of the Phen $\pi$-$\pi^*$ absorbance band ($\lambda_{max\ free}$: 268, $\lambda_{max\ bound}$: 274 nm)[10] with a clean isosbestic point at 272 nm, suggestive of a two-state process (Figure S3). All data were baseline-corrected and adjusted for dilution. Absorbance at 280 nm, which displays the largest change upon Ni binding, was plotted as a function of Ni concentration. The generated binding isotherm was fit to the following two-state equation[11] using IgorPro v. 4.0 (Wavemetrics, Inc.)

$$y = 0.5R\{A + B + x - \sqrt{(A + B + x)^2 - 4Bx}\}$$

where $R$ is $\Delta\varepsilon$ ($M^{-1}$ $cm^{-1}$), $A$ is $K_D$ (M), $B$ is [MBP-Phen1] (M), and $x$ is [Ni] (M).

**Crosslinking of MBP-Phen1 with lysine specific linkers dimethyl suberimidate (DMS), dimethyl pimelimidate (DMP), and dimethyl adipimidate (DMA) and ICP-OES/SV sample preparation** (Figures S4, S5, S6 and S8)

To a 0.5 mL solution containing 0.25, 0.5 or 0.75 mM MBP-Phen1 and $Ni^{2+}$ in 0.1 M HEPES buffer (pH 8) was added 10 μL of 0.3 M crosslinker (DMS, DMP or DMA, Pierce, Figure S4) in 0.1 M HEPES buffer (pH 8). Aliquots of the reaction mixture were taken out every 10 min and quenched with 0.1 M Tris (pH 8.5) for monitoring the progress of the reaction by SDS-PAGE electrophoresis. As a control, a parallel reaction was run under identical conditions that contained 5 mM EDTA instead of $Ni^{2+}$ to ensure a metal free environment. After 50 min,

any free crosslinker was quenched with 0.1 M Tris (pH 8.5), and the reaction mixture was analyzed by SDS-PAGE gel electrophoresis (Figure S6).

The resulting protein mixtures were purified by size-exclusion chromatography on an ACA54 resin (Pall), where the running buffer was 0.02 M Tris (pH 7) containing 100 μM $NiCl_2$ to prevent $Ni^{2+}$ dissociation during purification. The trimer thus isolated (<10 mL total volume) was dialyzed against 2×2 L of metal-free Tris buffer to remove unbound $Ni^{2+}$. The dialyzed product and an aliquot of the dialysis buffer were directly used for ICP-OES analysis (or for SV experiments after further concentration). The UV-vis spectrum of the isolated (and dialyzed) trimeric species (Figure S8) shows a maximum at 274 nm for the Phen group, which suggests that the majority of Phen groups in solution are bound to Ni.

**Crosslinking of MBP-Phen1 with $Ru^{2+}$ and ICP-OES/SV sample preparation** (Figures S7 and S8)

$Ru(DMSO)_4Cl_2$ was prepared as previously reported.[12] 2 mL of 1 mM MBP-Phen1 in 0.1 M HEPES (pH 7) and 1 equivalent of $Ru(DMSO)_4Cl_2$ were allowed to react under an inert Ar atmosphere for 4 days at room temperature. The reaction was stopped by removal of excess $Ru(DMSO)_4Cl_2$ via a DG-10 (BioRad) gel filtration column. The trimeric species was isolated via size-exclusion chromatography on an ACA54 resin (Pall), using 0.02 M Tris (pH 7) as the running buffer, and further purified on an Uno-Q anion-exchange column using an NaCl gradient. The isolated trimer (<10 mL total volume) was dialyzed against 2×2 L of metal-free Tris buffer to remove any unbound $Ru^{2+}$. The dialyzed product and an aliquot of the dialysis buffer were directly used for ICP-OES analysis (or for SV experiments after further concentration). Identity of the trimer fractions was determined using native-PAGE gel electrophoresis (Figure S7). The UV-vis spectrum of the isolated trimeric species (Figure S8) shows a maximum at 276 nm for the Phen group, which suggests that all Phen groups in solution are bound to Ru.

**Inductively coupled plasma-optical emission spectroscopy (ICP-OES) of Ru- and DMS-crosslinked MBP-Phen1** (Table S2)

Each MBP-Phen1 molecule contains a single Fe atom as a part of the covalently-attached heme group; therefore, the Ni:Fe and Ru:Fe ratios can be used to assign the oligomeric composition of the isolated species.

All chemicals used for ICP-OES experiments were of analytical grade and water was de-ionized in a Milli-Q system (resistivity of 18.2 MΩcm). All glassware and containers were rinsed 3× with 5% $HNO_3$. For standardization, a 30-mL solution containing 10 ppm of the metal analyte (Ni, Ru or Fe) was prepared by dilution from its certified 1000 ppm ICP stock solution (Ricca) with 5% $HNO_3$ in water. From this 10-ppm stock solution, 14 calibration solutions (0.0–5.0 ppm) were prepared by serial dilution. 4-mL solutions of crosslinked MBP-Phen1 species for analysis were prepared in a similar fashion in 5% $HNO_3$ and water. The Ni, Ru and Fe concentrations of the protein solutions were determined from their respective calibration curves. The ICP-OES results, as well as the specific wavelength used for the detection of each metal, are summarized in Table S2.

An inspection of both $Ni_3$:MBP-Phen1$_3$ crystal structures indicates that there is a low affinity coordination site for Ni near the N-terminus of every monomer. The coordination sphere of this internally bound Ni consists of the backbone N and O of Ala1 and the carboxylate sidechain of Asp39. To ascertain that this binding site does not contribute to the "Ni-count" for the DMS-crosslinked sample, we prepared a control sample of wild-type cytochrome $cb_{562}$ (which contains the low-affinity Ni site, but not the Phen groups for interprotein coordination) in

exactly the same fashion as the DMS-crosslinked sample. ICP-OES analysis of this species does not show any trace of Ni.

**Sedimentation Velocity** (Figures S9 and S10)

Sedimentation velocity (SV) experiments were performed in order to determine the solution-state oligomerization behavior of MBP-Phen1 (Figures S9 and S10). All SV samples were prepared in 20 mM Tris buffer (pH 7). Measurements were made on a Beckman XL-I Analytical Ultracentrifuge (Beckman-Coulter Instruments) using an An-60 Ti rotor at 41,000 rpm for a total of 250 scans per sample. The following wavelengths were used for detection: 425 nm (10 μM protein) and 650 nm (500 μM protein).

All data were processed using SEDFIT.[13] Buffer viscosity, buffer density, and protein partial specific volume values were calculated at 25° C with SEDNTERP (http://www.jphilo.mailway.com). Partial specific volume (Vbar) for MBP-Phen1 mutant was calculated to be 0.7344 mg/ml, assuming a partial specific volume of heme of 0.82 mg/ml and 0.71 mg/ml for the phenanthroline.[14] All data were processed using fixed values for buffer density (ρ) (0.99764 g/ml) and buffer viscosity (0.0089485 poise).

**Calculation of Theoretical Sedimentation Coefficients** (Table S3)

Theoretical sedimentation coefficients (Table S3) were calculated using HYDROPRO v. 7.0 as previously reported.[15] Hypothetical oligomerization conformations, such as the extended dimer (structure 7 in Figure S1b), and the extended trimer (structure 9), were modeled using PYMOL.[16] The closed dimer (structure 1) and closed trimer (structure 3) conformations were approximated using $Cu_2$:MBPC-$1_2$ (PDB ID: 3DE8) and $Ni_2$:MBPC-$1_3$ (PDB ID: 3DE9) structures, respectively.[17] All values for vbar (0.7344 $cm^3/g$), buffer density (0.99764 $g/cm^3$) and viscosity ($8.99 \times 10^{-3}$ P) were held constant.

**Crystallography** (Figures S11 and S12; Table S4)

All crystals were obtained by sitting drop vapor diffusion. MBP-Phen1 was crystallized at 25° C with a precipitant solution consisting of 100 mM Tris (pH 8.5), 200 mM NaCl (for the $P2_1$ crystals) or 200 mM $MgCl_2$ (for the $P6_322$ crystals), 25% PEG 2000, and 3.3 mM $NiCl_2$. The drop consisted of 2 μL protein (3.3 mM in 20 mM Tris, pH 7) and 2 μL precipitation solution. Crystals appeared within one month, reaching a maximum size of ~ 100 μm × 100 μm × 50 μm. The crystals to be used for diffraction experiments were exchanged into a solution containing 20% glycerol as a cryoprotectant and frozen in liquid nitrogen or directly in the cryostream.

X-ray diffraction data for both crystal forms were collected at 100 K at Stanford Synchrotron Radiation Laboratory (BL 9-1) using 0.97 Å radiation. The data were processed using MOSFLM and SCALA.[18] The structure of $Ni_3$:MBP-Phen$1_3$ was determined at 2.4 ($P2_1$ form) and 3.15-Å ($P6_322$ form) resolution, respectively, by molecular replacement with MOLREP, using the cyt c$b_{562}$ structure (PDB ID 2BC5)[1] as the search model. The search model for each crystal form did not contain the heme or the Phen prosthetic groups; the observation of strong positive $F_o$-$F_c$ density at expected positions for these groups confirmed the correct placement of protein monomers (12 in the $P2_1$ form and 2 in the $P6_322$ form) in the initial molecular replacement solutions. The topology and parameter files for the phenanthroline group were obtained using the Dundee ProDrg Server (http://davapc1.bioch.dundee.ac.uk/prodrg/index.html). Rigid-body, positional and thermal refinement with REFMAC,[18, 19] along with manual rebuilding, and water placement with XFIT,[20] produced the final models. For the $P6_322$ form, a two-fold non-crystallographic symmetry (NCS) restraint (tight main-chain and

medium side-chain restraints) was applied throughout the positional/thermal refinement process. Similarly, for the $P2_1$ form, a twelve-fold NCS restraint (tight main-chain and loose side-chain restraints) was applied throughout the refinement. In addition, for the latter crystal form, TLS refinement using each twelve monomers as rigid bodies was carried out during each refinement cycle. The Ramachandran plots were calculated with PROCHECK.[21] All figures were produced with PYMOL.[22]

Because the tunability of the beamline (SSRL BL9-1) we used is limited, we could not obtain anomalous diffraction data for the Ni centers. The fact that Ni is the only transition metal in crystallization solutions, and the refined B-factors for the modeled Ni-ions (on average: 32 $Å^2$ in $P2_1$ crystals, 31 $Å^2$ in $P6_322$ crystals) match well with those of the coordinating Phen groups (on average: 29 $Å^2$ in $P2_1$ crystals, 33 $Å^2$ in $P6_322$ crystals) gives strong credence to their assignment. The assignment for the diffuse electron density near Ni trans to the Phen group is somewhat less certain (Figures S11 and S12). The broadness of the electron density is most consistent with two atoms; therefore, two water molecules were initially modeled into this density. The average B-factors for the coordinated waters (which showed a ± 0.3 Å variation on their distance from the Ni ions, Figure S11e) after refinement were 28 $Å^2$ for the $P2_1$ crystals (24 waters) and 4 $Å^2$ for the $P6_322$ crystals. Since the lower thermal factors for coordinated ligands compared to Ni is not reasonable, we considered chloride ions as an alternative possibility. Both crystal forms emerged from solutions containing 200 mM $Cl^-$; all other possible candidates (PEG fragments, TRIS) were ruled out due to their shapes and sizes that are incompatible with the electron density. The average refined B-factors for coordinated $Cl^-$ ions were 58 $Å^2$ for the $P2_1$ crystals (24 ions) and 39 $Å^2$ for the $P6_322$ crystals. Based on these observations, we tentatively assign the electron density to a mixture of water and chloride ligands that are in rapid exchange. Although the observation of bound chloride ligands in an aqueous environment is unexpected, it is not without precedence.[23, 24]. For reporting purposes, the final submitted structure for the $P2_1$ crystals (3FOO) contains 24 water ligands, and that for $P6_322$ crystals (3FOP) contains 4 chloride ligands, for the sake of consistency with the observed B-factors.

As mentioned in the experimental section for the ICP-OES measurements, there is an internally coordinated Ni-ion for every MBP-Phen1 monomer not involved in any interprotein contacts. This Ni ion is coordinated to the N-terminal amine and the carbonyl oxygen of Ala1, and Asp39. Its identity was established in an earlier study on a similar Ni-mediated superstructure ($Ni_2$:MBPC-$1_3$) using anomalous diffraction data collected at the Ni K-edge.[17] The average B-factors for these Ni ions (66 $Å^2$ in $P2_1$ crystals, 52 $Å^2$ in $P6_322$ crystals) are significantly higher than those of the interfacial Ni ions (32 $Å^2$ in $P2_1$ crystals, 31 $Å^2$ in $P6_322$ crystals) or the protein atoms (41 $Å^2$ in $P2_1$ crystals, 43 $Å^2$ in $P6_322$ crystals), indicating that they are weakly bound.

**IR spectroscopy** (Figure S13)

Single crystals of $Ni_3$:MBP-Phen$1_3$ grown from a 25% PEG 2000, 100 mM Tris (pH 8.5), 200 mM $MgCl_2$, 3.3 mM $NiCl_2$ solution were soaked in 100 µL of the the mother liquor plus 20 µL of a 100 mM potassium cyanate (KNCO) solution to give a final concentration of 20 mM KNCO. As a control, "metal free" W59C-Phen, a mutant lacking His77, crystals were obtained in the presence of EDTA. Single crystals of W59C-Phen were soaked in 100 µL of their respective precipitation solution (2 M $NH_4SO_4$, 100 mM Tris (pH 8.5) with 3 mM EDTA) along with 20 mM KNCO. After 30 minutes of soaking, the crystals were cleaned off of excess KCNO. The crystals were then ground with KBr and compressed into a pellet. Infrared spectra were collected on a Bruker Equinox 55 FTIR spectrometer.

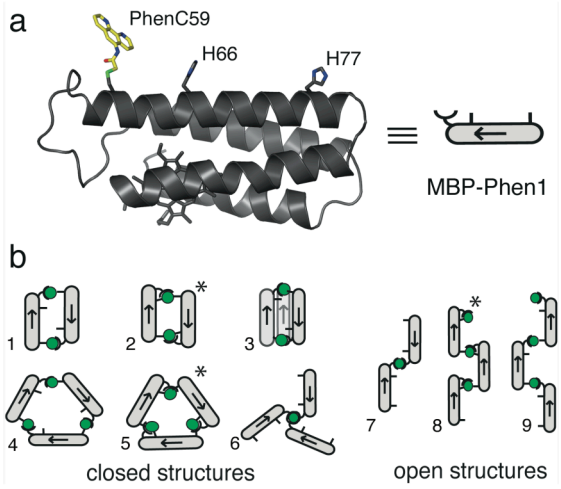


***Figure S1.*** (a) MBP-Phen1 structure with PhenC59 modeled in the extended form, and its cartoon representation. (b) Some possible Ni-induced oligomerization modes of MBP-Phen1, where each Ni ion is coordinated by at least one Phen group. Structures that feature *i*, *i* +7 His66-PhenC59 coordination of Ni are labeled with an asterisk.

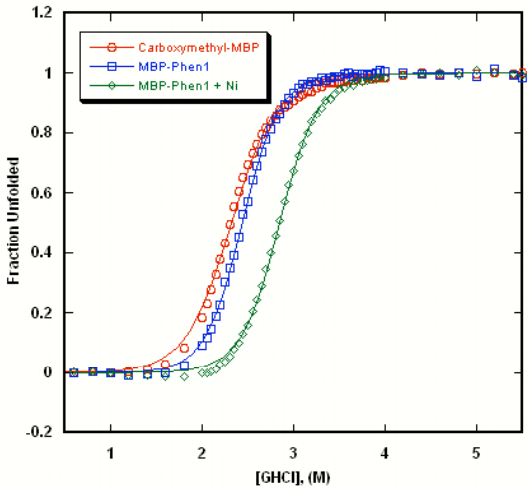


***Figure S2.*** GuHCl unfolding curves and fits for CM-MBP (with EDTA), MBP-Phen1 (with EDTA) and MBP-Phen1 (in the presence of 1 mM Ni(II)). The parameters obtained from the fits are listed in Table S1.

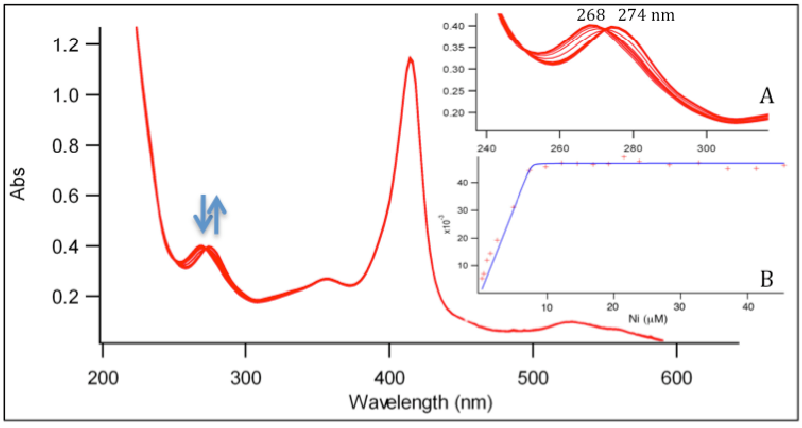


***Figure S3.*** Titration of MBP-Phen1 with Ni(II) as monitored by UV-vis spectroscopy. (Inset A) The red-shift of the phenanthroline $\lambda_{max}$ from 268 nm to 274 nm upon metal binding. (Inset B) Binding isotherm for MBP-Phen1 to Ni(II), fit to a two-state model (blue line), where (+) represents $\Delta A_{280\ nm}$. The shape of the isotherm confirms 1:1 Ni:Phen binding and indicates a $K_D < 1$ μM.

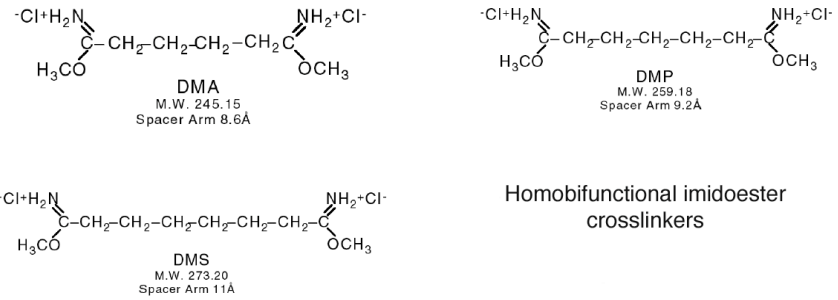


***Figure S4.*** Amine-reactive homobifunctional imidoester crosslinkers used in this study (Figure adapted from Pierce).

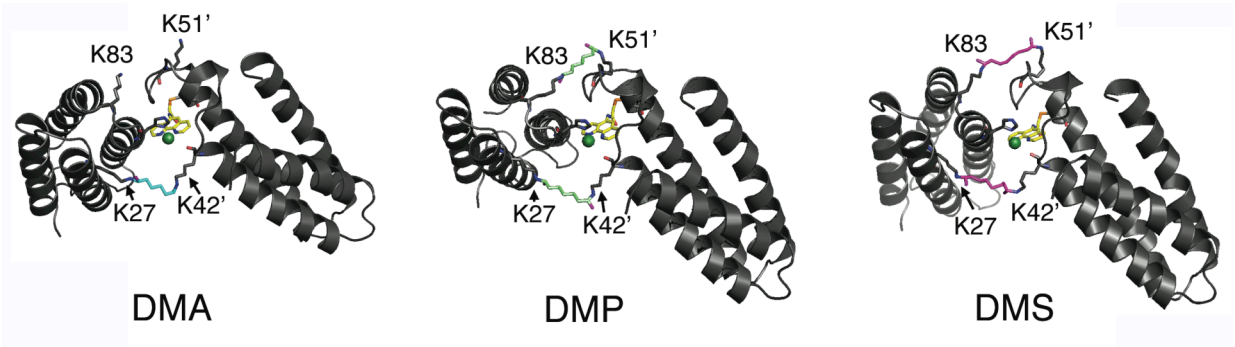


***Figure S5.*** Models for DMA/DMP/DMS-mediated crosslinking of K83-K51 and K27-K42 across crystallographically-observed monomer-monomer interfaces in $Ni_3$:MBP-Phen1$_3$ trimers. While the crosslinking of both Lys pairs appear to be readily accommodated (i.e., in low-energy, extended conformations of Lys, and no steric clashes with the intervening protein medium) with DMP and DMS, only the K27-K42 pair appears to be within reach for DMA.

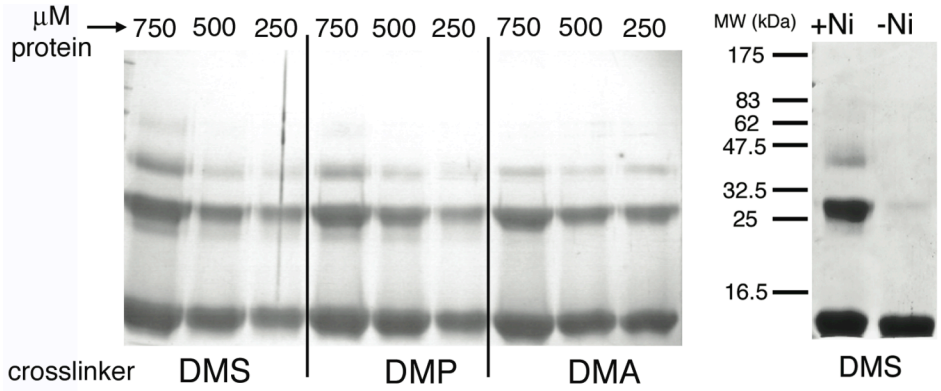


***Figure S6.*** (left panel) Concentration-dependent crosslinking of MBP-Phen1 by DMS, DMP and DMA in the presence of equimolar Ni as probed by SDS-PAGE electrophoresis. Crosslinking reactions were carried out using 250, 500 or 750 μM protein/$NiCl_2$ and 30-fold excess crosslinker at room temperature for 50 min. The monomeric mass is 12376 Da; the expected trimeric mass containing three DMS crosslinkers is 37737 Da. All crosslinkers yield dimeric, trimeric and some higher-order species in the presence of Ni; the yield of oligomeric species increases with crosslinker length. (right panel) The formation of oligomeric species is clearly metal dependent, as the yield for crosslinked dimeric and trimeric forms is markedly higher in the presence of Ni.

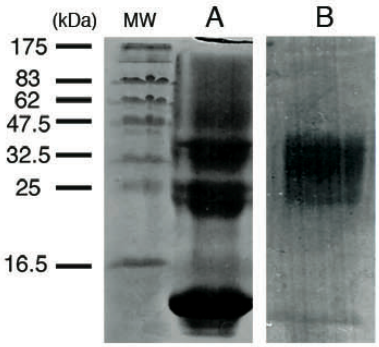


***Figure S7.*** 12% Native-PAGE gel of Ru-crosslinked MBP-Phen1 before (A) and after (B) purification. The broad band for the trimeric species indicates sample heterogeneity, which is also reflected by the somewhat broad sedimentation coefficient distribution (Fig S10).

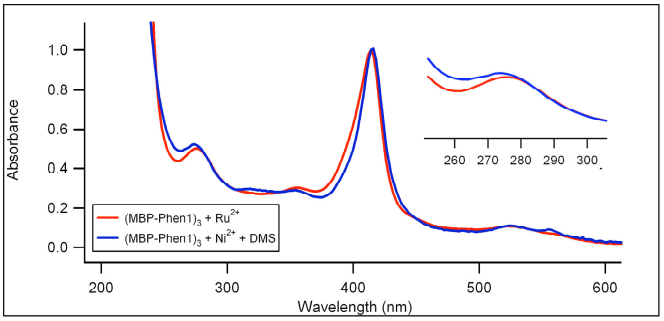


***Figure S8.*** UV-visible spectra of crosslinked trimeric species. Spectra of Ru(II)- (red) and DMS-crosslinked MBP-Phen1 in the presence of Ni(II) (blue) indicate that both species contain Phen groups that are fully metal-bound, with $\lambda_{max}$ = 276 nm and $\lambda_{max}$ = 274 nm for each species, respectively.

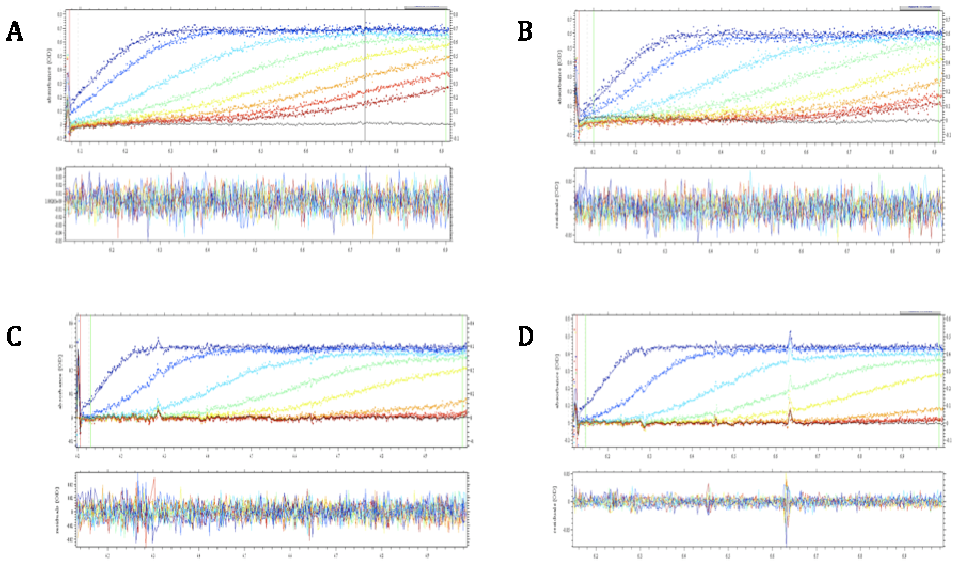


***Figure S9***. Sedimentation velocity data, fits and residuals for various MBP-Phen1 species. (A) 500 µM MBP-Phen1 in the presence of 1 mM EDTA ($f/f_0$ = 1.22, rmsd = 0.0135), (B) 500 µM MBP-Phen1 in the presence of 1 equivalent of Ni(II) ($f/f_0$ = 1.32, rmsd = 0.020), (C) 10 µM DMS-crosslinked MBP-Phen1 ($f/f_0$ = 1.29, rmsd = 0.0090), (D) 10 µM Ru-crosslinked MBP-Phen1 ($f/f_0$ = 1.41, rmsd = 0.0064).

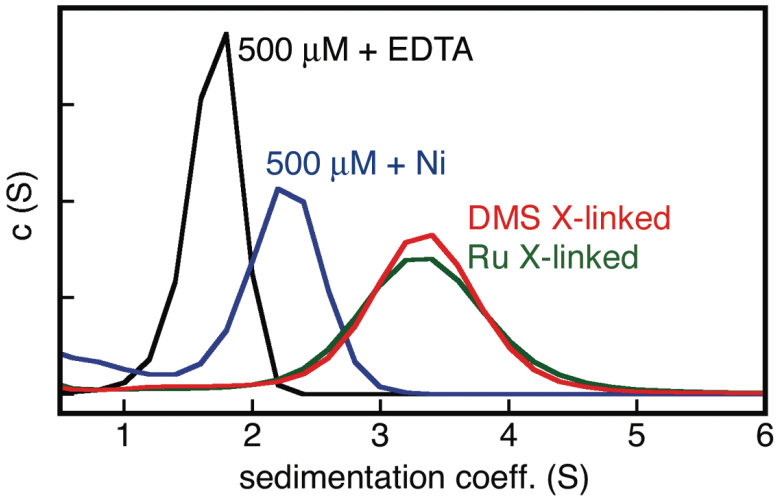


***Figure S10***. Normalized sedimentation coefficient distributions of MBP-Phen1 under various conditions. In the absence of Ni (black line), only the monomeric form is observed ($S_{max}$ = 1.8). The species with $S_{max}$ = 2.3 (blue line) obtained at 500 µM protein and Ni is most consistent with an extended dimeric species (expected $S_{max}$ = 2.4) such as structure 7 in Figure S1b. The population of the trimeric species in solution in significant quantities apparently requires high protein concentrations (> mM) such as those used for crystallization. Such MBP-Phen1 concentrations are not conducive to SV measurements due to the overwhelming intensity of heme absorption bands. As detailed in Table S3, $S_{max}$ = 3.3 observed for DMS- and Ru-crosslinked species is most consistent with a triangular species, whereas the theoretical sedimentation coefficients for the extended and the closed trimers (structures 8 and 3 in Figure S1b) are calculated to be 3.0 and 3.6 Svedbergs, respectively.

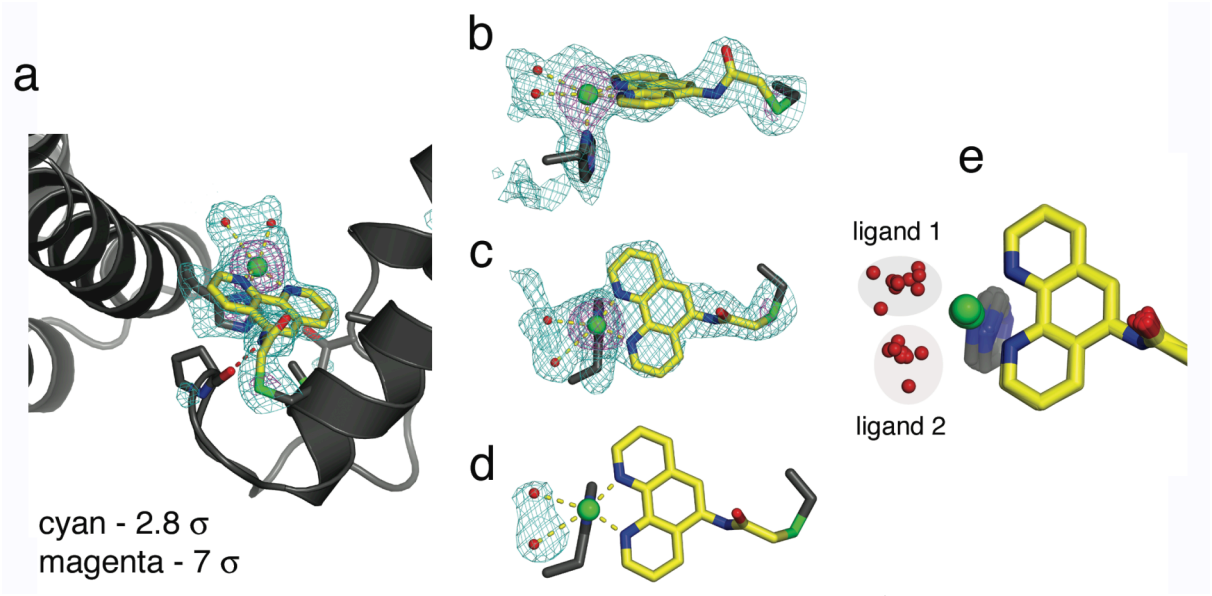


***Figure S11***. Close-up views of the Ni coordination environment in the 2.4-Å resolution $Ni_3$:MBP-$Phen1_3$ structure ($P2_1$ form). (a) The view corresponding to Fig.1 in the main text, showing the $F_o$-$F_c$ omit difference density maps calculated using a model where the Ni-center and the coordinating ligands were omitted (cyan mesh – 2.8 σ, magenta mesh – 7 σ). (b), (c) Side and topviews of the Ni coordination environment, and the corresponding $F_o$-$F_c$ omit difference density map. (d) $F_o$-$F_c$ omit difference density maps calculated using a model where only the coordinating ligands trans to Phen were omitted (cyan mesh - 3 σ). (f) Superposition of the Ni coordination environments in the twelve crystallographically independent monomers in the asymmetric unit, showing the variation in the position of the two non-proteinaceous ligands modeled as water molecules.

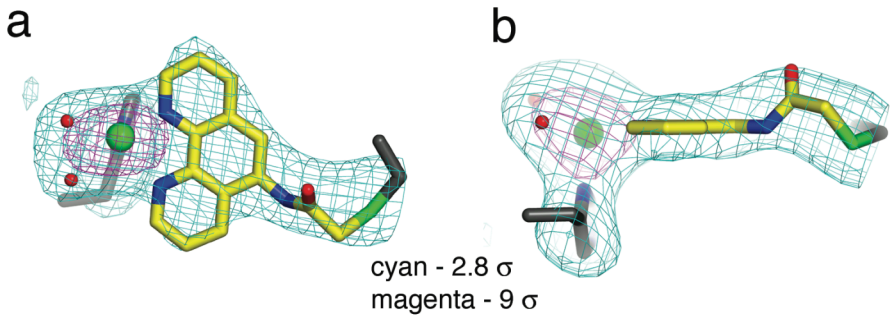


***Figure S12***. Ni coordination environment in the 3.15-Å resolution $Ni_3$:MBP-$Phen1_3$ structure ($P6_322$ form) and the corresponding $F_o$-$F_c$ omit difference density maps as viewed from the top (a) and the side (b).

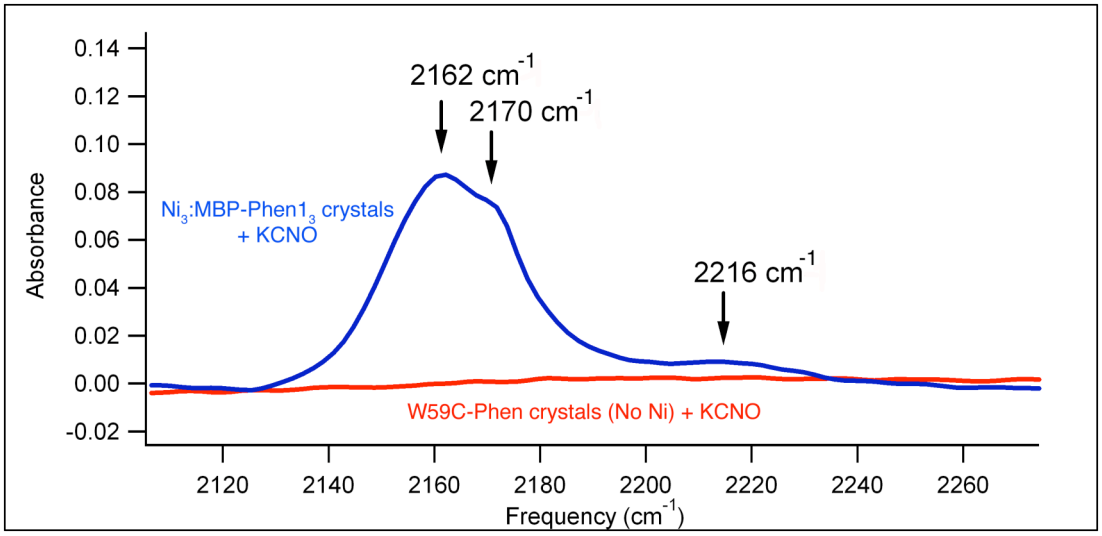


***Figure S13***. IR spectra of $Ni_3$:MBP-Phen1$_3$ and W59C-Phen crystals soaked in a 20 mM KNCO solution. Only the protein-transparent region of the IR spectrum is shown for clarity. W59C-Phen is a similar construct to MBP-Phen1 with the exception that it does not contain the His77 ligand. The crystals of W59C-Phen were grown in the presence of EDTA. The fact that no NCO stretching frequencies are observed for W59C-Phen crystals suggests that $NCO^-$ does not non-specifically associate with protein crystals. As a reference, the similar $Ni^{II}(terpy)(NCO)_2(H_2O)$ complex exhibits two asymmetric C-N stretching bands ($\nu_s$) at 2170 and 2230 $cm^{-1}$ attributed to two different modes of Ni-NCO interactions.[2] In comparison, the $\nu_s$ stretching frequencies for the $Ni(NCO)_4^{2-}$ complex and free $NCO^-$ are observed at 2196 $cm^{-1}$ and 2155 $cm^{-1}$, respectively.[4, 5]

A

| Carboxymethyl-MBP | Value |
|---|---|
| Mid-point (M of GuHCl) | 2.32 ±0.0052 |
| Slope ($kcal \cdot mol^{-1} \cdot M^{-1}$) | 2.34 ±0.048 |
| $\chi^2$ | 0.018 |
| R | 0.998 |

B

| MBP-Phen1 ($Ni^{2+}$) | Value |
|---|---|
| Mid-point (M of GuHCl) | 2.85 ± 0.0030 |
| Slope ($kcal \cdot mol^{-1} \cdot M^{-1}$) | 2.76 ± 0.034 |
| $\chi^2$ | 0.00498 |
| R | 0.999 |

C

| MBP-Phen1 (EDTA) | Value |
|---|---|
| Mid-point (M of GuHCl) | 2.43 ± 0.0023 |
| Slope ($kcal \cdot mol^{-1} \cdot M^{-1}$) | 2.875 ± 0.030 |
| $\chi^2$ | 0.00498 |
| R | 0.999 |

***Table S1.*** Parameters obtained from fits to the unfolding curves shown in Figure S2. The free energies for unfolding ($\Delta G_{unf}$) obtained from these parameters are 5.4 kcal/mol (CM-MBP), 7.0 kcal/mol (MBP-Phen1 in the absence of metal), and 7.9 kcal/mol (MBP-Phen1 in the presence of Ni).

DMS-crosslinked trimer

| Analyte (λ, nm) | Mean intensity | Conc. (mg/L) | Conc. µM |
|---|---|---|---|
| Ni (231.6) | 3932.0 | 0.145 (±0.0084) | 2.47 |
| Fe (238.2) | 7097.7 | 0.126 (±0.013) | 2.25 |
| Fe (239.56) | 7513.1 | 0.129 (±0.014) | 2.31 |

Ru-crosslinked trimer

| Analyte (λ, nm) | Mean intensity | Conc. (mg/L) | Conc. µM |
|---|---|---|---|
| Ru (349.89) | 23488.3 | 1.77 (±0.09) | 15.7 |
| Ru (240.27) | 27807.1 | 1.74 (±0.094) | 16.2 |
| Fe (238.2) | 42070.1 | 0.616 (±0.036) | 11.0 |
| Fe (239.56) | 42430.4 | 0.596 (±0.032) | 10.7 |

***Table S2***. ICP-OES metal analysis of dialyzed samples of DMS- and Ru-crosslinked MBP-Phen1 trimers. All samples were run in triplicate, and signals were corrected by subtraction of buffer background. These analyses yield a Ni:Fe ratio of 1.1 (± 0.1) and a Ru:Fe ratio of 1.4 (± 0.1). A control sample of wild type cytochrome $cb_{562}$ (not containing Phen) prepared in exactly the same fashion as the DMS-crosslinked species contains no Ni.

| MBP-Phen1 Conformation | Mw (Da) | Calculated sedim. coeff. (S) | Experimental sedim. coeff. (S) |
|---|---|---|---|
| Monomer | 12376 | 1.6 | 1.8 |
| Closed dimer (Structure 1) | 24752 | 2.67 | 2.6[a] |
| Extended Dimer (Structure 7) | 24752 | 2.46 | N/A |
| Closed Trimer (Structure 3) | 37128 | 3.56 | 3.5[a] |
| Extended Trimer (Structure 9) | 37128 | 3.0 | N.A |
| DMS-crosslinked $Ni_3$:MBP-$Phen1_3$ | 37737 | 3.26 | 3.3 |
| $Ru_3$:MBP-$Phen1_3$ | 37431 | 3.27 | 3.3 |

***Table S3.*** Various MBP-Phen conformations (as illustrated in Figure S1b), and their corresponding theoretical and experimental sedimentation coefficients. [a] From Reference 17.

| | $Ni_3$:MBP-Phen1$_3$ ($P2_1$) | $Ni_3$:MBP-Phen1$_3$ ($P6_322$) |
|---|---|---|
| Residues in complex | 3 × (106 + 1 Heme + 1 Phen + 2 Ni) | 3 × (106 + 1 Heme + 1 Phen + 2 Ni) |
| No. of complexes / asymmetric unit | 4 | 2/3 |
| Metal ions in asymmetric unit | 24 Ni (12 intersubunit/12 intrasubunit) | 4 Ni (2 intersubunit, 2 intrasubunit) |
| Waters in asymmetric unit | 119 | 21 |
| Unit cell dimensions (Å) | 70.3 × 107.4 × 102.1<br>$\alpha = \gamma = 90^\circ$, $\beta = 105.5^\circ$ | 104.9 × 104.9 × 107.9<br>$\alpha = \beta = 90^\circ$, $\gamma = 120^\circ$ |
| Symmetry group | $P2_1$ | $P6_322$ |
| Resolution (Å) | 98-2.4 | 90-3.15 |
| X-ray wavelength (Å) | 0.97 | 0.97 |
| Number of Unique Reflections | 55485 | 6496 |
| Redundancy | 2.7 (2.6) | 13.1 (13.4) |
| Completeness (%)* | 97.2 (97.0) | 100.0 (100.0) |
| $\langle I / \sigma I \rangle$* | 6.5 (1.3) | 5.2 (1.6) |
| $R_{sym}$‡ (%)* | 9.6 (55.2) | 13.6 (48.5) |
| R§ (%)* | 20.9 (27.1) | 21.2 (28.4) |
| Free R[II] (%)* | 26.8 (33.2) | 26.0 (39.8) |
| Rms Bnd[¶] (Å) | 0.009 | 0.014 |
| Rms Ang[¶] (°) | 1.25 | 1.49 |
| Ramachandran plot (%) | | |
| Residues in most favored regions | 97.3 | 96.4 |
| Residues in add.l allowed regions | 2.7 | 3.6 |
| Residues in generously allowed regions | 0.0 | 0.0 |
| Residues in disallowed regions | 0.0 | 0.0 |

**Table S4.** X-ray data collection and refinement statistics for $Ni_3$:MBP-Phen1$_3$.

‡ $R_{sym} = \Sigma\Sigma_j | I_j - \langle I \rangle | / \Sigma\Sigma_j | I_j |$.

§ $R = \Sigma | | F_{obs} | - | F_{calc} | | / \Sigma | F_{obs} |$.

[II]Free R calculated against 7.2 and 7.0% of the reflections removed at random for $P2_1$ and $P6_322$ crystals, respectively.

[¶]Root mean square deviations from bond and angle restraints.

*Numbers in parentheses correspond to the highest resolution shell: 2.53 – 2.40 Å and 3.32 – 3.15 Å for data collection, and 2.46 – 2.40 Å and 3.23 – 3.15 Å for refinement.

**References:**


1. Faraone-Mennella, J. T., F. A.; Gray, H. B.; Winkler, J. R., *Biochemistry* 2006, **45**, 10504-10511.
2. Cortes, R.; Arriortua, M. I.; Rojo, T.; Mesa, J. L.; Solans, X.; Beltran, D., *Acta Cryst. C* 1988, **44**, 986-990.
3. Braun, M. T.-M., L. , *Proc. Natl. Acad. Sci. USA* 2004, **101** 12830-12835.
4. Sabatini, A.; Bertini, I., *Inorg. Chem.* 1965, **4**, 959-&.
5. Nakamoto, K., Infrared and Raman Spectra of Inorganic and Coordination Compounds - Part B: Applications in Coordination, Organometallic and Bioinorganic Chemistry. 5 ed.; Wiley & Sons, Inc.: New York, 1997.
6. Castellano, F. N.; Dattelbaum, J. D.; Lakowicz, J. R., *Anal. Biochem.* 1998, **255**, 165-170.
7. Nozaki, Y., *Methods Enzymol.* 1972, **26**, 43-50.
8. Pace, N. C.; Shirley, B. A.; Thomson, J. A., In Protein Structure: A Practical Approach, Creighton, T. F., Ed. IRL Press: Oxford, 1990; pp 311-330.
9. Faraone-Mennella, J.; Tezcan, F. A.; Gray, H. B.; Winkler, J. R., *Biochemistry* 2006, **45**, 10504-10511.
10. Cheng, R. P.; Fisher, S. L.; Imperiali, B., *J. Am. Chem. Soc.* 1996, **118**, 11349-11356.
11. Stootman, F. H.; Fisher, D. M.; Rodger, A.; Aldrich-Wright, J. R., *Analyst* 2006, **131**, 1145-1151.
12. Evans, I. P.; Spencer, A.; Wilkinson, G., *J. Chem. Soc. Dalton Trans.* 1973, 204-209.
13. Schuck, P., *Biophys. J.* 2000, **78**, 1606-1619.
14. Calculated using Advanced Chemistry Development (ACD/Labs) Software V8.14 for Solaris (© 1994-2009 ACD/Labs).
15. de la Torre, J. G.; Huertas, M. L.; Carrasco, B., *Biophys. J.* 2000, **78**, 719-730.
16. DeLano, W. L., The PYMOL Molecular Graphics System (http://www.pymol.org). 2003.
17. Salgado, E. N.; Lewis, R. A.; Mossin, S.; Rheingold, A. L.; Tezcan, F. A., *Inorg. Chem.* 2009, **48**, 2726-2728.
18. Collaborative Computational Project, Number 4. 1994. "The CCP4 Suite: Programs for Protein Crystallography". Acta Cryst. D50, 760-763
19. Murshudov, G.; Vagin, A.; Dodson, E., *Acta Cryst.* 1996, **D53**, 240-255.
20. McRee, D. E., *J. Mol. Graphics* 1992, 44-46.
21. Laskowski, R. A., Macarthur, M. W., Moss, D. S., and Thornton, J. M., *J. Appl. Crystallogr.* 1993, **26**, 283-291.
22. DeLano, W. L. The PYMOL Molecular Graphics System (http://www.pymol.org), 2003.
23. Su, J. R.; Xu, D. J., *Acta Cryst. E* 2005, **61**, M1738-M1740.
24. Ding, C. F.; Miao, Y. F.; Tian, B. Q.; Li, X. M.; Zhang, S. S., *Acta Cryst. E* 2006, **62**, M1062-M1063.